Electric Conductivities of Alkali Metal Halides in Liquid Methanol along the Liquid–Vapor Coexistence Curve

Taka–aki Hoshina, Noriaki Tsuchihashi, Kazuyasu Ibuki, and Masakatsu Ueno*

Department of Molecular Science and Technology, Faculty of Engineering,
Doshisha University, Kyo–Tanabe, Kyoto 610-0321, Japan
*E-mail: mueno@mail.doshisha.ac.jp

The limiting ionic conductivities for the alkali metal and halide ions in methanol are reported and compared with the Hubbard–Onsager (HO) dielectric friction theory based on the continuum model along the liquid–vapor coexsistence curve at temperatures –15°C $\leq t \leq$ 240°C and the reduced densities 2.989 $\geq \rho_r \geq$ 1.506. At $\rho_r > 2.0$, the ionic friction coefficients in methanol are reproduced reasonably well by the HO theory. At $\rho_r < 2.0$, however, discrepancies between the theory and the experiment are obvious. Comparisons between the theory and the experiment are also carried out in water along the coexistence curve (25°C $\leq t \leq$ 350°C and 3.160 $\geq \rho_r \geq$ 1.821). In water, the theory cannot explain the ionic friction coefficients in the high density region where the effect of the hydrogen–bonded network is significant. At low densities where the charge effect is important, the HO theory works well in water.

1. Introduction

For a better understanding of the transport process in solutions, it is important to investigate the density effect over a wide range including the intermediate region between the liquid and the gas states; the continuum theory works well in the former state, while the binary–collision theory is valid in the latter. In order to attain such medium densities, elevated temperatures are necessary. In ionic solutions, the electric conductivity measurement is one of the most reliable methods to determine the ionic mobility. The electrolyte conductivities have been measured extensively at high temperatures in aqueous solutions [1,2] in which interesting properties arise from the effect of the hydrogen–bonded network. To disclose the general trends of the density dependence of ionic mobility at medium densities, and also to provide a reference to discuss the effect of the hydrogen–bonded network in aqueous solutions, the high temperature conductivity study should be extended to non–aqueous systems. Here we report the electric conductivities of the alkali metal ions (Na^+, K^+, and Cs^+) and the halide ions (Cl^-, Br^-, and I^-) [3,4] in liquid methanol along the liquid–vapor coexistence curve up to the critical temperature T_c = 513 K (240°C), and compare them with the results in aqueous solutions.

Methanol is a suitable solvent for the present purpose because the effect of the hydrogen–bonded structure is less important in methanol than in water; the three–dimensional hydrogen–bonded network is absent in methanol. Moreover, the solvent properties of methanol necessary for the discussion have been studied extensively in the subcritical region.

The sphere–in–continuum model is an appropriate reference model to discuss the general trend of the ionic dynamics at medium and high densities. At high liquid densities, the sphere–in–continuum model predicts the molecular transport properties reasonably well. Since the binary–collision model is valid at low densities, a break–down of the sphere–in–continuum model must be observed in the intermediate density region. One of the purposes of the present study is to discuss the validity of the sphere–in–continuum model in ionic solutions in the medium density region by comparing the experimental results with the Hubbard–Onsager (HO) dielectric friction theory [5,6].

2. Experimental Methods

The measurements of the molar conductivities Λ for NaCl, KCl, CsCl, KBr, and KI have been carried out in the temperature range of 60–240°C at pressures about 1 MPa higher than those on the

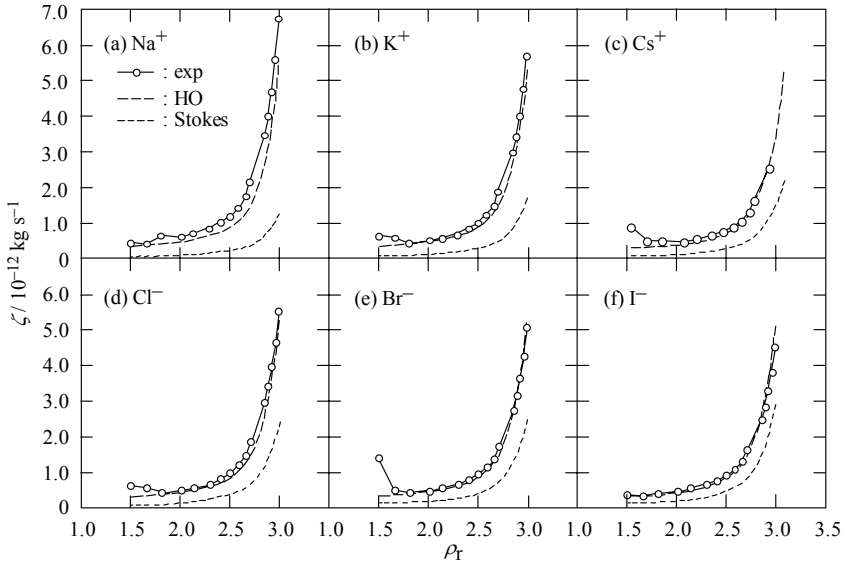

Fig. 1. Density dependences of the translational friction coefficients ζ for alkali metal ions and halide ions in liquid methanol along the liquid–vapor coexistence curve.

liquid–vapor coexistence curve. The equation of state for methanol is given by de Reuck and Craven [7]. The details of the experimental procedures are described in Ref. 3.

The concentration dependence of the molar conductivity Λ is analyzed by the Fuoss–Chen–Justice (FCJ) equation [8] with two fitting parameters, *i.e.*, the limiting molar conductivity Λ^0 and the molar association constant K_A. The FCJ equation is given by

$$\Lambda = \Lambda^0 - S\sqrt{\alpha c} + E\alpha c \ln(\alpha c) + J_1 \alpha c - J_2 (\alpha c)^{3/2} - \Lambda \alpha c f_\pm^2 K_A \ , \quad (1)$$

where α is the degree of dissociation and $f_\pm$ is the mean activity coefficient of the free ions. The detailed definitions of coefficients, S, E, J_1, and J_2 are given in Ref. 8 in terms of Λ^0, the dielectric constant ε, the viscosity η, the absolute temperature T, and the closest approach distance. For η [9] and ε [10], the values on the liquid–vapor coexistence curve are used in the analysis.

The limiting molar conductivities thus obtained are divided into the ionic contributions λ^0 by assuming that the limiting transference number t^0_+ of the K^+ ion in the KCl solution is independent of temperature and pressure at temperatures above 25°C. The t^0_+ value at 25°C and 0.1 MPa has been determined experimentally as $t^0_+ = 0.500$ [11]. The validity of the assumption has been discussed elsewhere [3].

The friction coefficient ζ is calculated from the ionic conductivity using the relation given by

$$\lambda^0 = \frac{z^2 eF}{\zeta} \ , \quad (2)$$

where F is the Faraday constant. The density dependences of the friction coefficients ζ obtained by eq. (2) are shown in Fig. 1. The reduced density ρ_r is defined as $\rho_r = \rho / \rho_c$, where ρ is the density and ρ_c (= 0.276 g cm^{-3}) the critical density of methanol. In this figure, the literature values of ζ at lower temperatures (25°C for the Cs^+ ion and –15°C < t < 25°C for the other ions) under atmospheric pressure [12,13] are also depicted.

3. Hubbard–Onsager Theory

We compare the experimental results with the Hubbard–Onsager (HO) theory based on the sphere–in–continuum model [5,6]. In the continuum theories, the translational friction coefficient is calculated from the hydrodynamic equation of motion for the solvent flow around a solute. For a neutral solute, the Navier–Stokes equation leads to the well–known Stokes law. The Stokes friction coefficient ζ_S for the slip boundary condition is given by

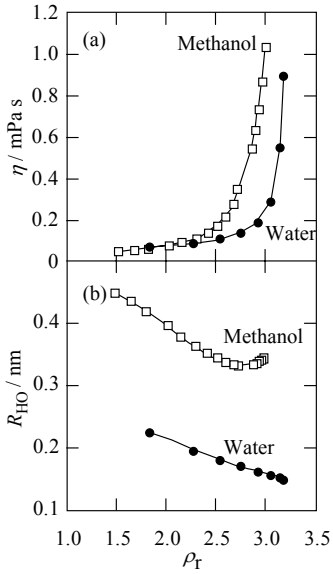

Fig. 2. Density dependences of (a) the viscosity and (b) the Hubbard–Onsager radius for methanol and water along the liquid–vapor coexistence curve.

$$\zeta_S = 4\pi\eta R, \tag{3}$$

where R is the ionic radius; the crystallographic radii by Pauling [14] are used as R in this study. The density dependences of the viscosities of methanol and water [15] along the liquid–vapor coexistence curve are shown in Fig. 2–(a). In both the solvents, the viscosity steeply decreases with decreasing density near the ambient condition.

For a charged solute which interacts with the solvent polarization, Hubbard and Onsager introduced an additional term to the Navier–Stokes equation and solved it to obtain the HO friction coefficient ζ_{HO} for an ion given in the form

$$\zeta_{HO} = \chi\eta R_{HO}, \tag{4}$$

where χ is the dimensionless friction coefficient which depends only on R/R_{HO}. The details of the theoretical calculation of χ are explained in Ref. 6, and an approximate expression for χ as polynomials in R/R_{HO} are given in Ref. 16. The solvent parameter called the HO radius R_{HO} is defined as

$$R_{HO} = \left[\frac{(ze)^2(\varepsilon - \varepsilon_\infty)\tau_d}{64\pi\eta\varepsilon_0\varepsilon^2}\right]^{1/4}. \tag{5}$$

Figure 2–(b) shows the density dependence of R_{HO} for methanol along the liquid–vapor coexistence curve. The high–frequency dielectric constants ε_∞ are estimated from the polarizability with the aid of the Lorenz–Lorentz equation. The dielectric relaxation times τ_d are taken from Hiejima *et al*. [17]. As seen in Fig. 2–(b), R_{HO} of methanol increases with decreasing density except for the most highest density region. This indicates that the effect of the dielectric friction increases with decreasing density.

The density dependence of R_{HO} of water [18] is also exhibited in Fig. 2–(b). The R_{HO} values of water are much smaller than those of methanol, while the density dependences show a similar tendency.

4. Results and Discussion

4.1. Ion–size Dependence The ion–size dependences of the ionic friction coefficient for the alkali metal and the halide ions in methanol in three conditions are shown in Fig. 3. The ionic friction coefficients are normalized to that for the K^+ ion in each condition.

In ambient condition, Fig. 3–(a), the experimental friction coefficient decreases with increasing ion–size for both of the alkali metal and the halide ions, while the ion–size dependences for the cations and anions are not smoothly connected. The Stokes law predicts the ion–size effect in the direction opposite to the experimental results indicating the importance of the charge effect. The friction coefficient predicted by the HO theory is independent of the sign of the ionic charge and its ion–size dependence is smaller than the observed one.

At lower densities down to $\rho_r = 2.0$ (t = 200°C), the ion–size dependence of the experimental friction coefficient becomes smaller as shown in Fig. 3–(b); the experimental friction coefficients are indeed nearly independent of the ion–size at ρ_r = 2.0 and t = 200°C except for the Na^+ ion. The HO theory explains the ion–size dependence of the friction coefficient more successfully at lower densities and high temperatures.

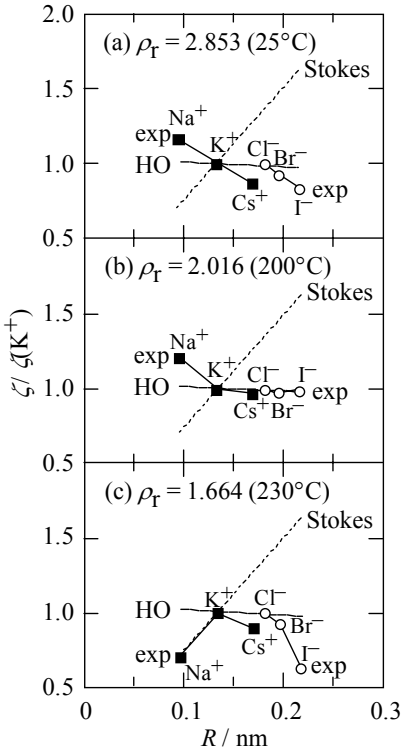

Fig. 3. Ion–size dependences of the ionic friction coefficients normalized to that of K^+ ion for the alkali metal ions and the halide ions in liquid methanol along the liquid–vapor coexistence curve.

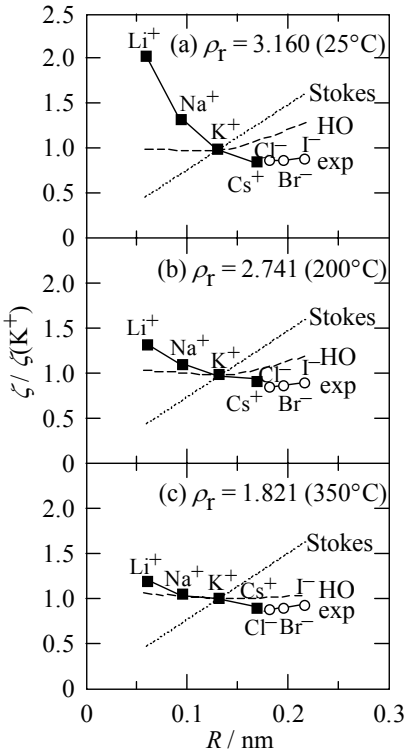

Fig. 4. Ion–size dependences of the ionic friction coefficients normalized to that of K^+ ion for the alkali metal ions and the halide ions in water along the liquid–vapor coexistence curve.

At ρ_r = 1.66 (t = 230°C), the ion–size dependences of the experimental friction coefficients for the halide ions are again much larger than the prediction of the HO theory as shown in Fig. 3–(c). For the alkali metal ions, the ion–size dependences of the experimental and the HO friction coefficients are in the opposite direction. This indicates that such a low density as ρ_r = 1.66 is out of the validity range of the HO theory in methanol.

The ion–size dependences of the ionic friction coefficient for the alkali metal ions and the halide ions in water in three conditions are shown in Fig. 4. The experimental data for the ionic conductivities along the coexistence curve are taken from Oelkers and Helgeson [2].

In ambient condition, Fig. 4–(a), the experimental friction coefficients of the alkali metal ions decrease with increasing the ionic radius, while those of halide ions increase slightly. Although the existence of the minimum in the ion–size dependence of the friction coefficient is predicted by the HO theory, the predicted ion–size dependence is much smaller than the experimental one for the alkali metal ions and much larger for the halide ions.

As the density decreases down to ρ_r = 1.8 (t = 350°C), the ion–size dependences of the experimental friction coefficients become smaller as shown in Figs. 4–(b) and (c). At ρ_r = 1.8 (t = 350°C), the ion–size dependence of the experimental friction coefficients is close to the prediction of the HO theory. This indicates that the ion–size dependence is well explained by the HO theory at high temperatures and low densities in water. As far as the ion–size dependence of the ionic friction coefficient is concerned, qualitatively similar results are obtained in methanol and water.

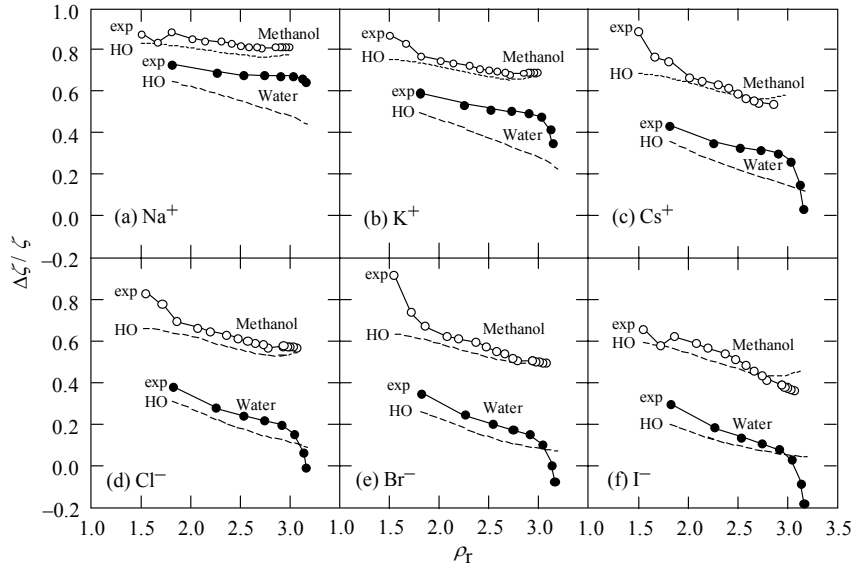

Fig. 5. Density dependences of the relative residual friction coefficients $\Delta\zeta/\zeta$ for alkali metal ions and halide ions in liquid methanol and water along the liquid–vapor coexistence curve.

4.2. Density Dependence As shown in Fig. 1, the ionic friction coefficients in methanol decrease steeply with decreasing density in the high density region for all the ions studied. Although the drastic density dependences of the viscosities dominate those of the friction coefficients, it is clear from the discrepancies between the experiment and the Stokes law that the ionic friction coefficients cannot be explained exclusively by the viscosity effect. The HO theory, on the other hand, shows a reasonable agreement with the experiment indicating the importance of the dielectric friction effect.

For detailed comparisons between the experiment and the HO theory, the relative residual friction coefficient $\Delta\zeta/\zeta$ is estimated. The residual friction coefficient $\Delta\zeta$ is defined by the following equation:

$$\Delta\zeta = \zeta - 4\pi\eta R. \tag{6}$$

The density dependences of the relative residual friction coefficients in methanol are shown in Fig. 5. For all the ions studied, the experimental results of $\Delta\zeta/\zeta$ increase with decreasing density, and the prediction of the HO theory agrees with the experimental results nearly quantitatively in the density range of $\rho_r > 2.0$ ($t < 200$°C). This indicates that the effect of the dielectric friction is significant and well explained by the HO theory in medium–density methanol. At $\rho_r < 2.0$, however, the experimental results of $\Delta\zeta/\zeta$ are much larger than the prediction of the HO theory except for the Na^+ and I^- ions. This indicates that the application limit of the HO theory lies at about $\rho_r = 2.0$ in methanol.

The density dependences of $\Delta\zeta/\zeta$ in liquid water are shown in Fig. 5 in addition to those in methanol.

The experimental results of $\Delta\zeta/\zeta$ for the six ions in water are much smaller than those in methanol. The solvent effect on $\Delta\zeta/\zeta$ is well explained by the HO theory.

In contrast to the results in methanol, the discrepancies between the experiment and the HO theory are obvious in water at high densities. The HO theory underestimates $\Delta\zeta/\zeta$ of the cations around $\rho_r = 3.0$, and cannot explain the observed steep density dependences of $\Delta\zeta/\zeta$ of the large ions at $\rho_r > 3.0$. The limitations of the HO theory in high–density water in which the dielectric friction effect is weak are ascribed to the effect of the three–dimensional hydrogen–bonded network in water.

At low densities, the predicted values of $\Delta\zeta/\zeta$ by the HO theory become closer to the experimental ones with decreasing density for all the ions studied in water. Since the screening of the charge effect by the solvent dielectric is much weaker at lower densities, the dielectric friction effect is more significant and the HO theory is more reliable. It has been shown at temperatures higher than the present ones [18] that the HO theory works well in water at densities down to $1.4\rho_c$ which is lower than the application limit in methanol. At present we have no clear explanation for the

difference between the application limit densities in water and in methanol. The present results suggest, however, that the high hydrogen–bonded ability of water may induce many–body interactions at medium densities extending the validity range of the continuum model. Note that the hydrogen–bonded network in sub– and supercritical water is not in the tetrahedral geometry similar to ambient water but in the chain–like one [19,20] similar to methanol [21]. Further studies in a variety of solvents are necessary.

5. Conclusions

In this paper, we have reported the limiting ionic conductivities for the alkali metal and the halide ions in methanol and examined the validity of the Hubbard–Onsager dielectric friction theory based on the sphere–in–continuum model at temperatures between –15°C and 240°C along the liquid–vapor coexistence curve; the corresponding range of the reduced density is $2.989 \geq \rho_r \geq 1.506$. The density and the ion–size dependences of the friction coefficient are explained reasonably well by the HO theory at $\rho_r > 2.0$, although in ambient condition, the ion–size dependence of the friction coefficient is somewhat smaller than the observed one. At density lower than $\rho_r = 2.0$, however, discrepancies between the HO theory and the experiment are obvious. We have also compared the theory and the experiment in water at temperatures between 25°C and 350°C along the coexistence curve ($3.160 \geq \rho_r \geq 1.821$). In water, the theory cannot explain the ionic friction coefficients in the high density region; this result may be ascribed to the effect of the hydrogen–bonded network. When the density is decreased, however, the density and ion–size dependences of the friction coefficient predicted by the HO theory agree well with the experimental ones in water indicating the significant dielectric friction effect at low densities.

Acknowledgements

The authors are grateful to Professor M. Nakahara of Kyoto University for inspiring discussion and encouragements.

References

[1] P. C. Ho, H. Bianchi, D. A. Palmer, and R. H. Wood, *J. Solution Chem.*, **29**, 217 (2000), and the references cited therein.
[2] E. H. Oelkers and H. C. Helgeson, *J. Solution Chem.*, **18**, 601 (1989).
[3] T. Hoshina, N. Tsuchihashi, K. Ibuki, and M. Ueno, *J. Chem. Phys.*, **120**, 4355 (2004).
[4] T. Hoshina, K. Tanaka, N. Tsuchihashi, K. Ibuki, and M. Ueno, *J. Chem. Phys.*, **121**, 9517 (2004).
[5] J. B. Hubbard and L. Onsager, *J. Phys. Chem.*, **67**, 4850 (1977).
[6] J. Hubbard, *J. Phys. Chem.*, **68**, 1649 (1978).
[7] K. M. de Reuck and R. J. B. Craven, *Methanol, International Thermodynamics Tables of the Fluid State* (Blackwell, Oxford, 1993), Vol. 12.
[8] J.–C. Justice, In *Comprehensive Treatise of Electrochemistry*; ed. by B. E. Conway, J. O'M. Bockris, and E. Yeager (Plenum, New York, 1983), Vol. 5, Chap. 3, p. 310.
[9] N. B. Vargaftik, *Tables on the Thermophysical Properties of Liquid and Gases*, 2nd Ed., translated by Y. S. Touloukian (Hemisphere Pub., Washington, 1975).
[10] W. Dannhauser and L. W. Bahe, *J. Chem. Phys*., **40**, 3058 (1964).
[11] J. A. P. Davis, R. L. Kay and A. R. Gordon, *J. Chem. Phys*., **19**, 749 (1951).
[12] R. L. Kay and D. F. Evans, *J. Phys. Chem*., **70**, 2325 (1966).
[13] J. Barthel, M. Krell, L. Iberl, and F. Feuerlein, *J. Electroanal. Chem.*, **214**, 485 (1986).
[14] L. Pauling, *The Nature of the Chemical Bond*, 3rd Ed. (Cornell University, Ithaca, 1960).
[15] *JSME Steam Tables*, The Japan Society of Mechanical Engineering (2000) (in Japanese); based on the IAPWS Industrial Formulation 1997 for the Thermodynamic Properties of Water and Steam.
[16] K. Ibuki and M. Nakahara, *J. Chem. Phys*., **84**, 2776, 6979 (1986).
[17] Y. Hiejima, Y. Kajihara, H. Kohno, and M. Yao, *J. Phys*.: *Condens. Matter*, **13**, 10307 (2001).
[18] K. Ibuki, M. Ueno, and M. Nakahara, *J. Mol. Liq*., **98/99**, 124 (2002).
[19] N. Matubayasi, C. Wakai, and M. Nakahara, *J. Chem. Phys*., **107**, 9133 (1997).
[20] J. Martí, *J. Chem. Phys.*, **110**, 6876 (1999).
[21] N. Asahi and Y. Nakamura, *J. Chem. Phys.*, **109**, 9879 (1998).